JOURNAL OF MATERIALS SCIENCE 6 (1971) 427–438

Some Aspects of the Fracture of Boron-Aluminium Composites

P. W. JACKSON, A. A. BAKER*, D. M. BRADDICK
Rolls-Royce Ltd (Aero-Engine Division), Old Hall, Littleover, Derby, UK

A variety of mechanical tests has been performed on boron-aluminium composites. The fracture behaviour has been studied using both conventional metallography and the scanning electron microscope. The relationship between the structural characteristics of the composite, the mechanical properties and mode of testing, and the observed fracture behaviour are discussed.

1. Introduction

Fibre reinforcement provides a method for strengthening metals and alloys [1, 2]. Much of the early experimental work used in the formulation of the basic strengthening theories was performed using metal wires. More recently various ceramic fibres, such as glass, carbon, boron and sapphire, have become available and have been incorporated into metal matrix composites [3-6].

One of the most interesting composites from a technological viewpoint consists of boron fibres, prepared by the continuous chemical vapour deposition of boron on to a tungsten wire substrate, distributed within a matrix of aluminium or aluminium alloy. A considerable amount of work has been put into the development of boron fibres with a consistent diameter and high strength, followed by the development of suitable fabrication techniques to enable the full potential of the fibre to be utilised in composites [7-10].

Extensive mechanical property data have been accumulated, with much of the earlier work mainly relating tensile strength to fabrication conditions. More recently, rather more comprehensive evaluations of mechanical properties have been reported [6-12] and some attention has also been given to fracture mechanisms under various conditions [6, 11, 13, 14).

The present work was undertaken with the purpose of obtaining a balanced picture of some typical boron fibre/aluminium matrix composite material and also exploring some of the fractures in more detail with the aid of the scanning electron microscope.

A small quantity of boron/aluminium composite material was purchased from Harvey Aluminium Company, Torrance, California, USA. This was in the form of sheets nominally 1 and 2.5 mm thick respectively. The sheets were fabricated by laying up the fibres between foils of the matrix and consolidating by a diffusion bonding process. The matrix chosen was 6061 alloy (1% Mg, 0.6% Si, 0.25% Cu, 0.25% Cr, balance Al), which has the additional advantage of being amenable to heat treatment with a consequent improvement in both longitudinal and transverse composite strength [7-9].

Tests were performed on the material in two conditions, (a) as-received, (b) heat treated (H/t). The heat treatment consisted of annealing at 500°C for 1 h followed by a water quench, with subsequent ageing at 170°C for 6 h. The mechanical tests included longitudinal and transverse tensile, flexural and impact properties, reversed bending fatigue and high amplitude tension/tension fatigue. The relevant details of each mechanical test are described more fully in the appropriate sections below.

Post testing examination of fractures was performed using optical metallography of polished sections and also, more directly, by scanning electron microscopy of fracture faces. A Cambridge "Stereoscan" instrument was used, with the stage set at an angle of 40°. Specimens were coated with an evaporated film of gold approximately 500 Å thick before examination to minimise charging effects.

2. Initial Composite Characterisation

The specific gravity of two small composite

*Now at Department of Metallurgy, University of Nottingham.

samples was determined by both mensuration and displacement of ethylene dibromide. Both samples gave almost identical results, 2.61 by mensuration and 2.66 by displacement. These results confirm that there is little porosity in the composite, since the SG of the boron fibre (making due allowance for the tungsten wire substrate) is about 2.58 and the SG of 6061 aluminium alloy is about 2.70. The volume fraction of fibres (V_f) was determined gravimetrically by dissolving the matrix out of two samples using dilute hydrochloric acid. The results were 44.9 and 46.1 wt % fibres respectively, equivalent to 46.1 and 48.2 vol % fibres.

A sample of the as-received composite was cross-sectioned and polished. The distribution of the fibres was found to be reasonably uniform, with only a small amount of fibre/fibre contact, although there was a noticeable tendency for the fibres to remain in layers because of the composite fabrication technique.

No trace of the bond between adjacent matrix foils was observed in the as-polished sample, although this was subsequently revealed by heavy etching. The random internal longitudinal radial cracking which is a feature of boron filaments [15] was also apparent in the polished cross-section.

The surface structure of the boron filaments themselves is illustrated in fig. 1 which was obtained from a boron filament extracted by dissolution of the matrix in dilute hydrochloric acid. This "corn-cob" structure is typical for filaments prepared by this chemical vapour deposition route. The picture also shows that the good fibre/matrix bond is not obtained at the expense of excessive chemical reaction between fibre and matrix, since there is no pitting evident on the fibre surface. Fig. 2, taken from a transverse tensile fracture surface (see 4.1 below) illustrates the boron fibre's propensity for forming longitudinal radial cracks.

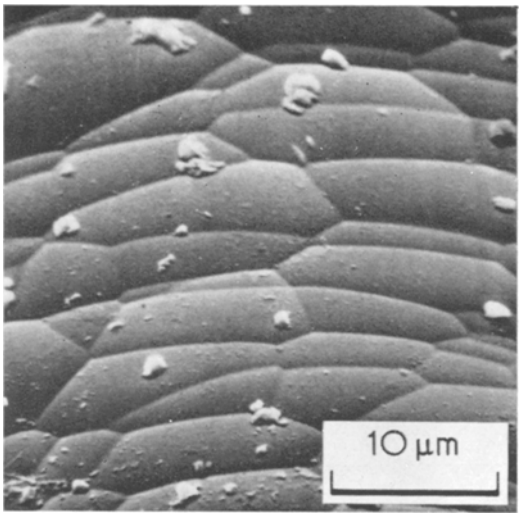

Figure 1 Boron fibre, extracted by dissolution of Al matrix.

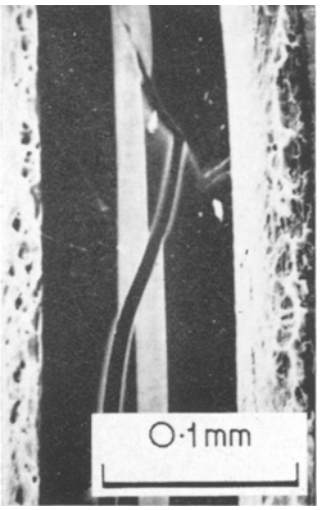

Figure 2 Longitudinal fracture of boron fibre.

3. Longitudinal Properties

3.1. Tensile

Checks were performed using an Instron tensile testing machine on the tensile modulus of specimens in both the as-received and heat-treated conditions, with either extensometers or strain gauges. Values ranging from 205 to 240 GN/m²* were obtained, from which the most accurate values appeared to be ~225 GN/m², which agrees reasonably well both with the predicted rule-of-mixtures value and also previously reported data [6].

Two specimens in each condition were necked down to give a parallel gauge length of ~20 mm and width ~6 mm. Stress/strain to failure curves were then obtained using the 10 mm extensometer. Typical curves are shown in fig. 3. The UTS values are given in table I and appear in reasonable agreement with predictions based on "rule of mixtures" and also well within the spread of results reported in the literature [6-8].

"Stereoscan" pictures of tensile fracture surfaces are shown in fig. 4 and illustrate the

*1 GN/m² ≡ 145,000 lb/in²

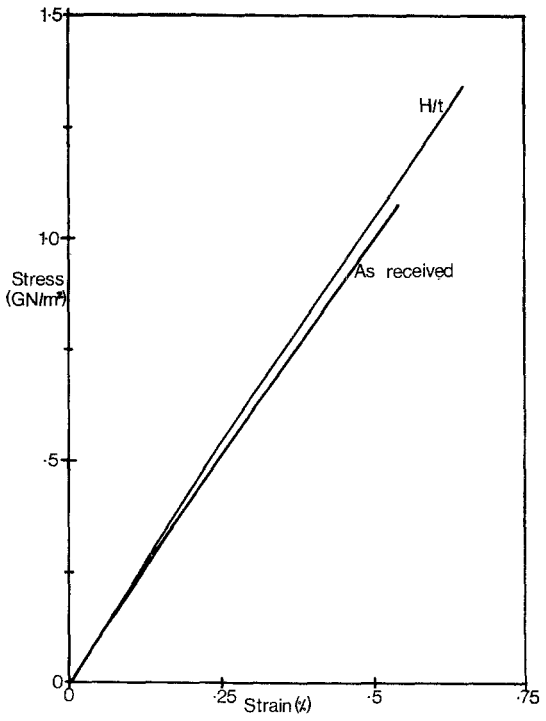

Figure 3 Longitudinal stress/strain behaviour.

extremely good bonding present in the composite obtained during the diffusion bonding manufacturing process. No traces are visible of the boundaries between individual matrix foils. The fibre/matrix bonding is also very strong as demonstrated by the very small amount of fibre pull-out visible on the fracture surface.

Most fibres have fractured flush with the surrounding matrix; even shattered fragments of fibre, formed during a secondary fracture next to the original fibre break, remain in their position firmly stuck to the surrounding matrix. The majority of the fibres show fractures initiating from internal defects, generally at the highly stressed core, giving rise to the characteristic conical fracture surface. Considerable ductility has been exhibited by the matrix on the fracture surface, particularly in the as-received specimens.

TABLE I UTS

Condition	UTS (GN/m^2)	Elongation (%)	Comments
As-received	1.06, 1.08	0.6, 0.54	Difference between conditions is significant only at 5% level because of
H/t	1.23, 1.34	0.6, 0.65	few data

3.2. Flexural

The dynamic flexural modulus was measured by a sonic method using a resonant beam technique. The sample dimensions were 100 × 12.5 × 1 mm. Mean values of 213 GN/m^2 were obtained for both the as-received and the heat-treated composites.

The flexural strength was determined from tests on specimens of size 45 × 5 × 1 mm. Three-point bending was performed over a 38 mm span, giving an l/d ratio of ~ 40, the load being applied through 12.5 mm diameter rollers. Flexural strengths were calculated from

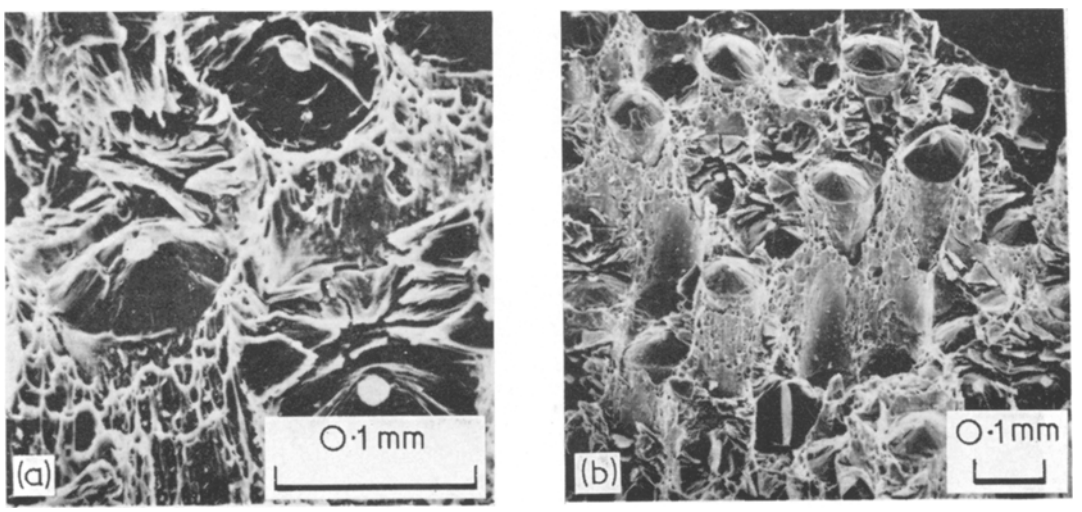

Figure 4 Longitudinal tensile fracture surfaces. (a) as-received B-Al, (b) H/t B-Al.

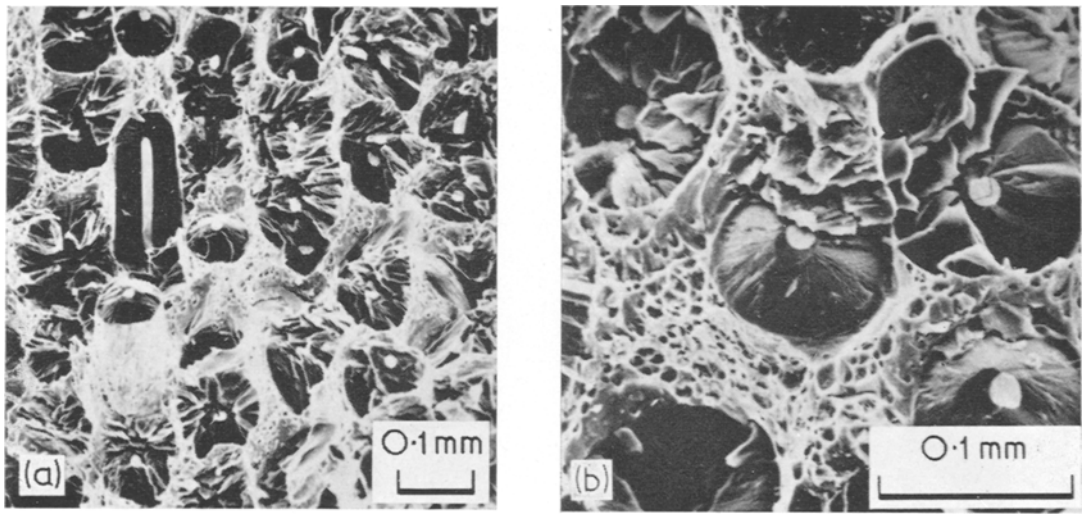

Figure 5 Flexural fracture surfaces. (a) as-received B-Al, (b) H/t B-Al.

$$\sigma = \frac{3Fl}{2b\,d^2}$$

where σ = flexural strength, F = load applied to central roller, l, b, d = test span, specimen width and thickness respectively. Results are shown in table II.

TABLE II Longitudinal flexural strength.

Condition	Longitudinal flexural strength (GN/m^2)	Mean LFS	Comments
As-received	1.48, 1.61, 1.64, 2.01, 2.07	1.77	Insufficient data to show significant difference between conditions.
H/t	1.65, 1.68, 2.17, 2.33	1.96	

"Stereoscan" pictures of fracture surfaces are shown in fig. 5. No signs of interlaminar shear failure were evident in any of the specimens and generally the fractures were very similar to the tensile fractures illustrated in fig. 4. A few longitudinally-split fibres were encountered, as illustrated in fig. 5; even these pulled-out portions of fibre still had matrix firmly adhering to their outer surface. Fig. 5b also contains a fibre showing a central brittle crack running through the core and out to link with cracks on the fibre fracture face.

3.3. Impact

Since only a limited amount of material was available, these tests were performed on small-scale specimens. A small Hounsfield plastics impact machine was used since a certain amount of background experience existed with reinforced plastics and other materials. The test-specimen shape and orientation is illustrated in fig. 6a. The measured impact values are given in table III. For comparison, a typical value for a high strength aluminium alloy in this test is $\sim$ 0.25-0.3J*.

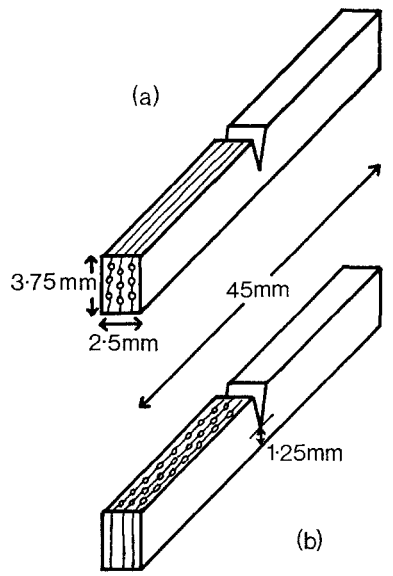

Figure 6 Impact test-pieces. (a) longitudinal, (b) transverse.

*1 J ≡ 0.738 ft. lb.

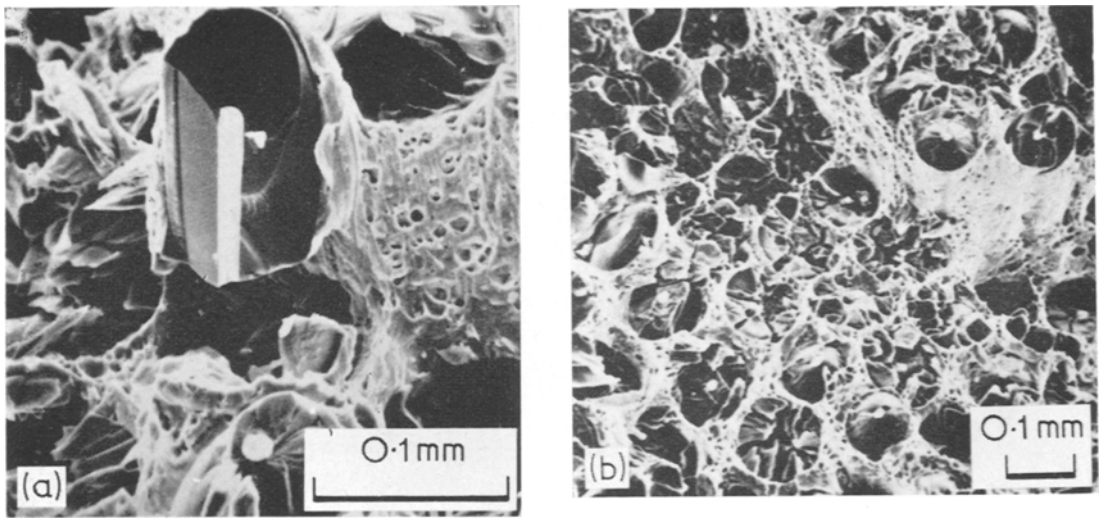

Figure 7 Longitudinal impact fracture surfaces. (a) as-received B-Al, (b) H/t B-Al.

TABLE III Longitudinal impact.

Condition	Energy absorbed (J)	Comments
As-received	0.088, 0.095, 0.100, 0.102	Insufficient data
H/t	0.081, 0.084, 0.091, 0.095	to show significant difference between conditions.

"Stereoscan" pictures of longitudinal impact fractures are shown in fig. 7. These fractures exhibit the same general characteristics as the longitudinal tensile and flexural fractures shown in figs. 4 and 5, i.e. good fibre/matrix bond with no signs of fibre pull-out and considerable matrix ductility, particularly in the as-received composites. However, these impact fractures differ considerably from the "static" fractures in showing a very much larger amount of fragmented fibre (still attached to the matrix – further evidence of the strong fibre/matrix bond) deriving from the high energy dissipated by the impact.

4. Transverse

4.1. Tensile

Specimens in both as-received and heat-treated condition were necked down to provide a parallel gauge length of ~ 20 mm with a width of ~ 5 mm. Stress/strain to failure curves were then obtained using the 10 mm extensometer. Typical results are shown in the graph, fig. 8. The additional transverse stiffening and strengthening resulting from the heat treatment is very pronounced, although data on this composite in the literature [9] claim that transverse strengths as high as 214 MN/m² can be obtained. The initial modulus before yielding, the transverse UTS and the strain at the UTS are shown in table IV.

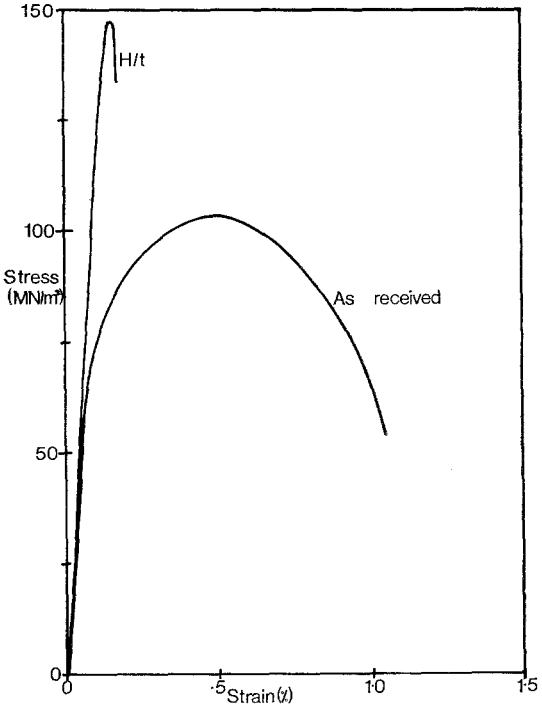

Figure 8 Transverse stress/strain behaviour.

Metallographic examination of a section taken through the fracture face of an as-received specimen showed that the fracture path, in addition to travelling through the matrix, split

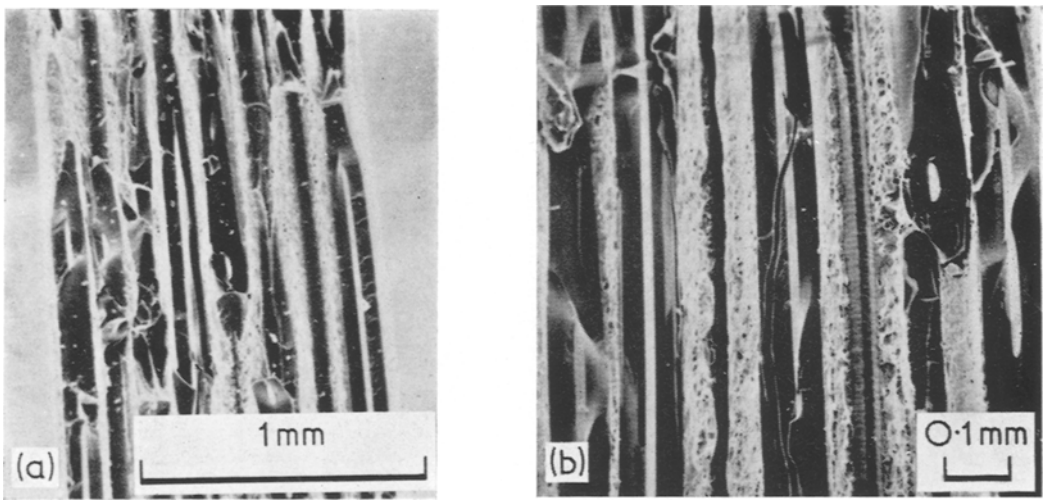

Figure 9 Transverse tensile fracture surfaces. (a) as-received B-Al, (b) H/t B-Al.

TABLE IV Transverse modulus, UTS and strain.

Condition	Transverse modulus (GN/m^2)	Transverse UTS (MN/m^2)	Strain at UTS (%)	Comments
As-received	109	103 110 } Mean 110 111 113	0.52 0.36 — 0.37	Significant difference between conditions despite few data (UTS—1% level, strain—5% level)
H/t	116	148 150 } Mean 149	0.15 0.20	

some boron fibres longitudinally (presumably when the pre-existing cracks were suitably oriented) and sometimes followed the fibre/matrix interface instead. This behaviour was confirmed by the "Stereoscan" examination (fig. 9). The fracture of a heat-treated composite appeared very similar to the as-received, although during examination it appeared that the proportion of split fibres was higher, although this was not easy to confirm. This examination confirmed that the longitudinal radial cracks continue unimpeded through the central core of the filaments, thus supporting the argument that the core is no longer a tungsten wire, but has reacted to form a tungsten boride, W_2B [15] (also see fig. 2).

4.2. Flexural

The transverse sonic modulus was measured as previously described in 3.2. The sample dimensions were 100 × 50 × 1 mm (with the fibres running in the 50 mm direction). The results were 127, 132 and 151 GN/m^2, giving a mean transverse sonic modulus of 135 GN/m^2. These are in good agreement with other experimental results which were fitted to an analytical model [16].

TABLE V Transverse flexural strength.

Condition	1/d Ratio	Transverse flexural strength (MN/m^2)	Comments
As-received	6.5	263	Difference between conditions is only significant at 5% level because of few data.
	16	234	
H/t	6.5	309	
	15	315	

Transverse flexural strengths were measured on specimens with the fibres across the sample width. Three-point bend tests were performed on a 15 mm span (4 mm diameter rollers) on specimens of nominal width 5 mm and thickness 1 mm and 2.5 mm respectively. The results are given in table V. The generally high level of these properties is apparent and the effect of heat treatment in boosting these transverse properties is particularly clear.

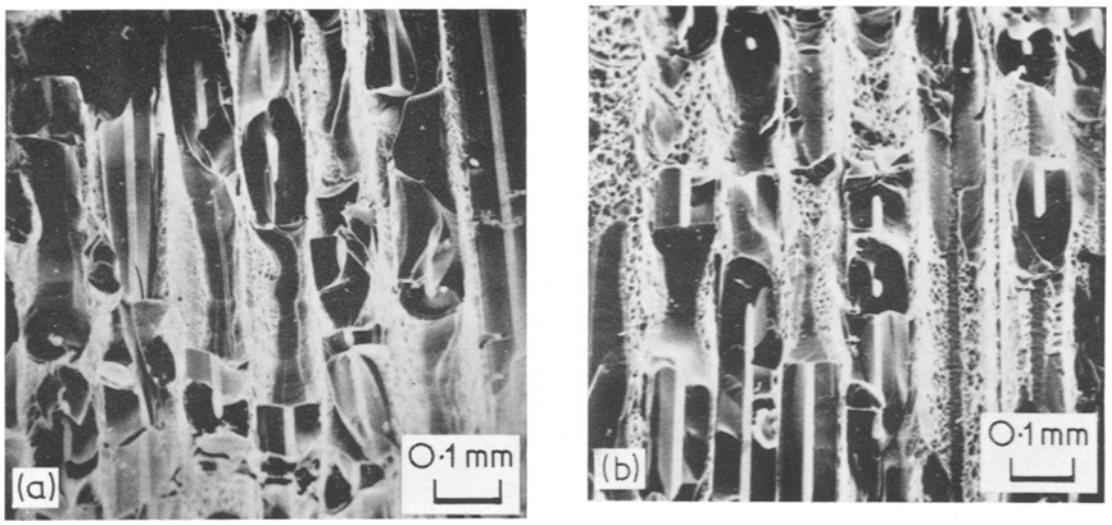

Figure 10 Transverse impact fracture surfaces. (a) as-received B-Al, (b) H/t B-Al.

TABLE VI Transverse impact.

Condition	Energy absorbed (J)	Comments
As-received	0.019, 0.020, 0.023, 0.026	No significant difference between conditions.
H/t	0.014, 0.0155, 0.0285, 0.030	

Transverse impact tests were performed in the same manner as the longitudinal impact tests (as described in 3.3), but on specimens machined as in fig. 6b. The "down-the-fibres" impact mode was selected because of the material thickness available and probably represents the most pessimistic transverse failure mode. The measured impact values are given in table VI.

"Stereoscan" pictures of transverse impact fractures are shown in fig. 10. The fractures generally show the same characteristics as the transverse tensile fractures in fig. 9, i.e. the fracture path runs through the ductile matrix, longitudinally-split fibres and through the fibre/matrix interface. However, the fracture path is very much more irregular and there is a high degree of shattering evident in the split fibre – a feature that is common to the longitudinal impact fractures.

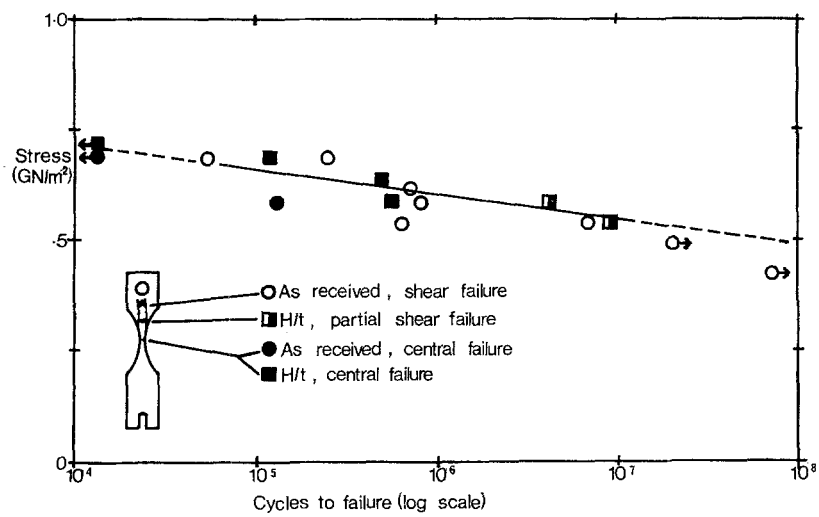

Figure 11 Reversed bending fatigue.

5. Fatigue

Testing was performed in reversed bending at constant stress, using the 50 Hz electromagnetic vibrator apparatus previously employed on aluminium matrix composite studies [17, 18]. Both as-received and heat-treated samples were evaluated. The specimen shape and individual mode of failure are indicated in fig. 11 (inset), along with the S/N curve constructed from the results. The nearly flat curve obtained agrees well with previously reported data on B-Alcomposites [7, 8], although the present results are at a slightly lower stress level and in addition there is no noticeable tendency for the heat-treated composites to give slightly inferior results.

The lower stress/high endurance specimens, particularly the as-received samples, tended to fail in a manner involving considerable shear cracking of the specimen, as illustrated on the inset sketch in fig. 11. The propagation of fatigue shear cracks through the matrix near a specimen surface is shown in the longitudinal taper section of fig. 12.

The high stress/low endurance specimens tended to fail in the waisted region of the specimen close to the section at nominal maximum stress. This tendency was particularly marked in the heat treated specimens. "Stereoscan" pictures of fractured specimens are shown in fig. 13. It is noteworthy that, in contrast to the tensile and flexural tests, the fibre fractures are often relatively flat, with much fewer fibres showing evidence of the characteristic conical

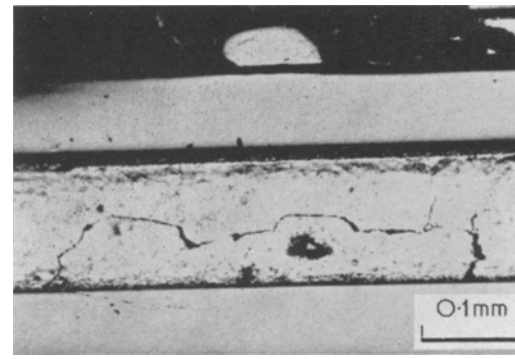

Figure 12 Longitudinal taper-section through high endurance fatigue fracture (as-received B-Al).

fracture. Although the matrix itself has been distorted to some extent by the compressive portion of the cycling, some interesting features emerge, for instance fibre/matrix debonding and matrix/matrix interlayer debonding (fig. 13b). This kind of interface and matrix failure was only observed after fatigue tests. Fig. 13a illustrates where a matrix crack opened up (apparently *not* at the matrix/matrix bonding interface) close to the central shear plane of a specimen. The propagation of a fatigue crack through a fibre in a heat treated specimen is illustrated in the longitudinal taper section of fig. 14, which also shows some matrix fatigue cracks developed from a cracked fibre.

A few additional high amplitude fatigue tests were conducted using the Instron testing machine at a frequency of approximately 20 to 30

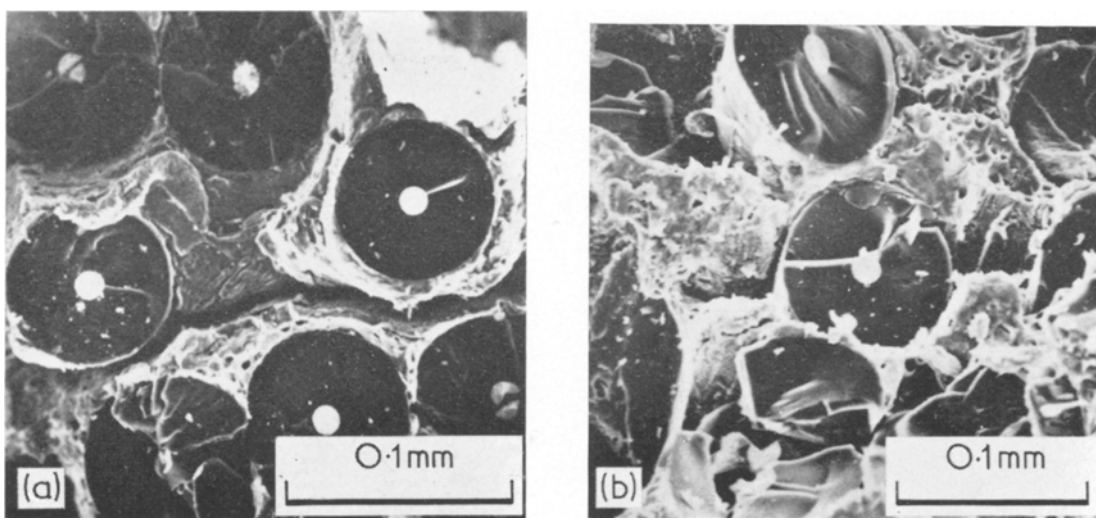

Figure 13 Fatigue fracture surfaces. (a) as-received B-Al, low endurance, (b) H/t B-Al, low endurance.

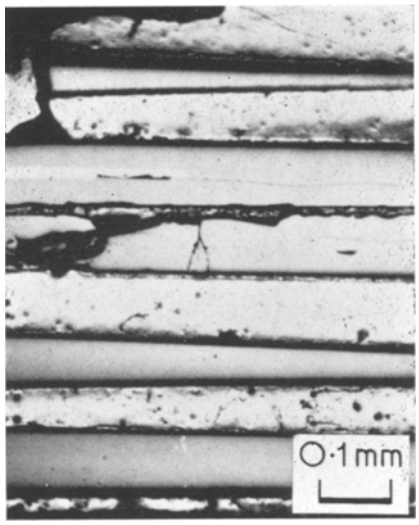

Figure 14 Longitudinal taper-section through low endurance fatigue fracture (H/t B-Al).

cycles/min. In order to examine fracture surfaces that were undistorted by a partially compressive cycle, the test modes were tension/tension and also three-point bend cycling, which has the additional advantage of localising the initial fatigue region to near the tensile face. This was particularly useful, since in high amplitude tension/tension testing it proved very difficult to distinguish between the fatigue and tensile failure areas on the fracture face.

The propagation of a fatigue crack through a three-point bend specimen is shown in fig. 15 (the two photographs overlap). A further example of a relatively flat fibre fracture is shown in fig. 15a. A fatigued portion of the matrix between fibres is shown enlarged in fig. 16a with a further example of matrix fatigue striations close to a fibre/matrix interface in fig. 16b. These matrix striations may be compared with the more usual matrix ductile failure mode as shown in fig. 17, which is from another part of this specimen. Fig. 17 does, however, show fatigue cracks starting in the surface of the specimen, as well as providing two excellent examples of conical (i.e. core-initiated) failures in the boron fibres.

6. Discussion

B-Al composites have several characteristics which interact to determine the composite's responses to a variety of test conditions. These characteristics include:

(*a*) completely elastic fibre with high modulus and high tensile strength;

(*b*) a marked tendency for fibre failure to initiate from internal flaws at or near the core and for the fibres to contain longitudinal radial cracks;

(*c*) a strong fibre/matrix interfacial bond, apparently achieved without a damaging degree of chemical interaction;

(*d*) fully ductile aluminium alloy matrix which is capable of further strengthening by heat treatment;

(*e*) large monofilament fibre which permits precise lay-up during fabrication and facilitates the realisation of the full fibre strength in the

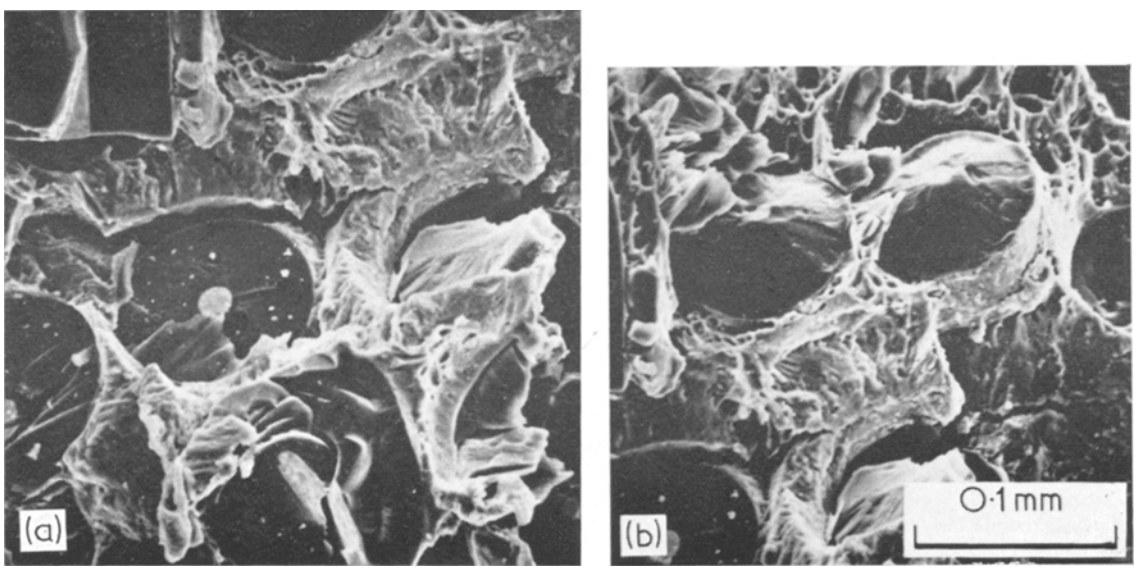

Figure 15 Fatigue fracture propagation (three-point bend, H/t B-Al, low endurance).

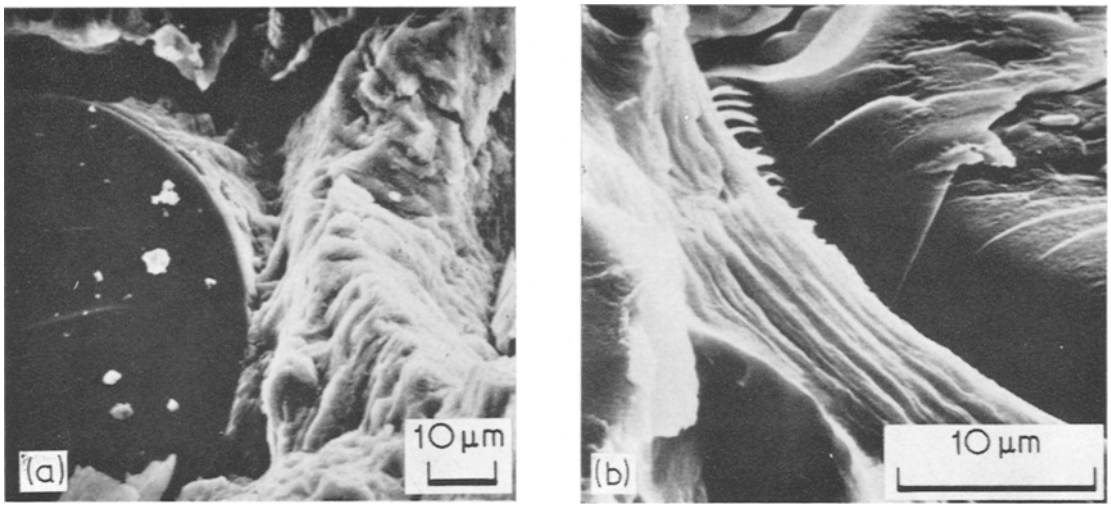

Figure 16 Fatigue fracture propagation, (three-point-bend, H/t B-Al, low endurance).

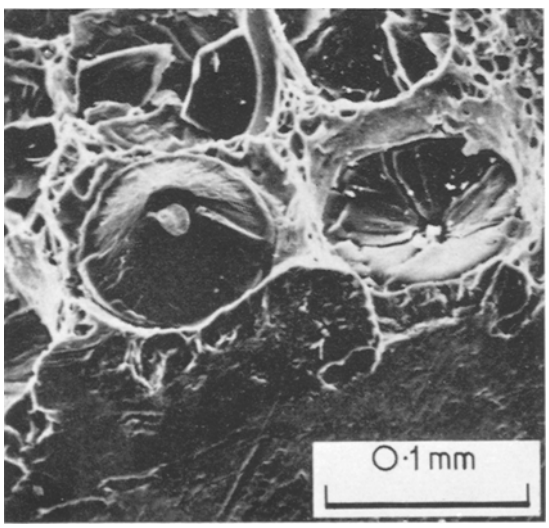

Figure 17 Fatigue specimen failure, showing tensile failure and matrix fatigue cracks.

composite.

The effects of these characteristics are shown quite clearly in the mechanical test results and in the resultant fracture behaviour. The near-linear longitudinal stress-strain behaviour, with a slight reduction in slope once the matrix yield stress has been exceeded, is illustrated in fig. 3 and follows the pattern to be expected from a fully continuous elastic fibre in a ductile matrix. The longitudinal tensile strength levels obtained in the samples suggest that a high proportion of the original fibre tensile strength is being utilised, confirming that the fabrication process has been successful in avoiding significant fibre damage. The noticeable increase in tensile strength resulting from heat treatment confirms more extensive results reported by other workers [7, 8]. This increase was also apparent in the longitudinal flexural tests, although it is perhaps unwise to compare the absolute flexural strength values directly with the tensile results because of the inevitable uncertainty in the stress distribution in a flexural test, particularly in a composite containing an inelastic component.

As expected, the longitudinal tensile and flexural fracture faces (figs. 4, 5) appeared very similar when examined on the "Stereoscan", because the flexural specimens failed through the propagation of a crack from the tensile face. In both test conditions the bulk of the fibres themselves failed from flaws associated with the core rather than the fibre outer surface. This is further confirmation of the lack of fibre damage associated with the strong fibre/matrix bond, which is itself demonstrated by the very small amount of fibre pull-out apparent. Even so the occasional fibres which stick up from the fracture face seem to have a thin layer of matrix adhering to them, since the "corn-cob" structure is not readily visible on the side of the fibres.

The strong fibre/matrix bond, particularly in the heat-treated samples, is also apparent in the way in which fibre fragments, created by the characteristic double-cone fracture typifying centrally-originated failure, have been retained bonded to the matrix at the fracture site (see fig. 5). Fracture of the matrix material itself has

occurred in a fully ductile manner involving the coalescence of microvoids. Comparison of the as-received and the heat-treated fractures shows that the amount of deformation (i.e. localised ductility) has been somewhat greater in the as-received samples.

As anticipated from previous studies on silica-aluminium composites [19], the impact tests have demonstrated that the energy-absorbing capacity of the composite is strictly limited. The elastic behaviour of the fibres dominates the impact behaviour, with the strong fibre/matrix bond preventing energy absorption by delamination and fibre pull out and also localising plastic deformation within the composite to the region of the matrix at the fracture surface. For this reason, although the matrix ductility can be altered by heat treatment, the effect of this on the overall energy-absorbing properties of the composite appears insignificant. The fracture faces (fig. 7) in addition to showing the features found on the longitudinal tensile and flexural faces, also showed a very high proportion of fragmented filaments, suggesting that multiple fibre fractures had occurred close to the fracture surface as a consequence of the impact loading. The manner in which these fragments have adhered firmly to the surrounding matrix is further dramatic confirmation of the strength of the fibre/matrix bond.

The transverse properties of the composite are dominated by (a) the strong aluminium alloy matrix (particularly in the heat-treated condition), (b) the strong fibre/matrix bond and (c) the presence of longitudinal radial cracks in the boron fibres themselves, resulting from reaction during fibre manufacture converting the tungsten core to tungsten boride. The effects of heat treatment are particularly apparent in the improvements in tensile and flexural properties, although no significant differences were apparent in the fracture faces (fig. 9). As would be anticipated the fracture path follows a line roughly parallel with the fibres with no real sign of fibre longitudinal tensile failure. The fracture face shows failure to have occurred via longitudinally split fibres and the fibre/matrix bond, linked via failure across the ductile matrix. Internal fibre flaws appear to be the main limitation to further improvements in transverse strength rather than the strength attainable by the matrix itself.

The transverse impact tests have confirmed the low energy-absorbing capacity of this composite, although in comparison with resin matrix composites the transverse impact properties are good, because of the relatively high transverse tensile strength and the influence of the ductile matrix in not permitting a completely brittle fracture mechanism. The main features of the fracture faces (fig. 10) are similar to the transverse tensile failures, but there is a striking difference in the disorderly manner in which the split fibres and broken fibre/matrix bonds have been linked. Coupled with this feature is the tendency for many of the fibres to remain as small pieces, still attached to the matrix, suggesting that a certain amount of multiple fracturing has occurred within each filament, in a similar manner to that observed with the longitudinal impact samples.

Fatigue testing introduces many new features to the fracture characteristics. Tests on single boron filaments [20] have shown that the fatigue resistance of boron filaments is high although a fatigue effect was observed. No evidence is available concerning fatigue fractures, nor of the mechanism of boron fibre fatigue. The primary fatigue effects in the B-Al composite would therefore be anticipated from matrix and interfacial fatigue effects.

High endurance fatigue tests resulted in extensive matrix cracking including matrix/matrix and fibre/matrix interfacial debonding. Significant amounts of interfacial debonding of this sort were not observed during tensile and flexural testing and it is interesting to note how effective fatigue is at exposing slightly weak interfaces, a result which has been noted previously in fatigue studies on silica-aluminium composites [17].

Under high stress/low endurance conditions, the tensile proportion of the final fracture increased. Nevertheless the increased proportion of flat fibre fractures (a characteristic of surface-initiated failure) compared with tensile and flexural tests suggests that fatigue cracks in the matrix induce some premature failures in the fibres, possibly by introducing stress concentrations at the tips of the matrix fatigue cracks. This behaviour may be qualitatively predicted from the high yield stress of the matrix and the high fibre/matrix bond strength [18, 21]. Figs. 14 and 15a support this view in showing flat fibre fractures which lie directly in the path of the advancing matrix fatigue crack. The tendency for a matrix crack to cause some fibre failure is further indicated by the tendency of the heat-treated samples, tested in reversed bending, to

fail by complete sample separation in the region of nominal maximum stress. This behaviour is markedly different from the as-received samples which most often failed with a rather indeterminate shearing type of fracture.

The actual fatigue fracture strain in the composite is similar to the fatigue fracture strain of the unreinforced matrix, e.g. for a fatigue stress of ~ 600 MN/m^2 and a composite modulus of ~ 225 GN/m^2, the strain is $\sim 2.5 \times 10^{-3}$. For 6061 aluminium alloy, a life of $\sim 5 \times 10^6$ cycles would be expected at a stress of ~ 140 MN/m^2 which, assuming a matrix modulus of ~ 70 GN/m^2, gives a similar strain of $\sim 2 \times 10^{-3}$. It is hoped to consider these results in more detail and also the effect of fatigue testing at elevated temperature in a further paper.

7. Summary and Conclusions

B-Al composites have been examined and their mechanical properties and fracture behaviour assessed under a variety of test conditions. The bulk of the test data and fracture characteristics correlated well with the physical characteristics of the composite. For example, the high longitudinal tensile and flexural strengths confirmed the retention of high fibre strength in the composite, whereas the relatively high transverse strengths confirmed the strong fibre/matrix bond. The impact data confirmed the absence of a mechanism for the absorption of a large amount of energy, since delamination was not observed and plastic deformation was confined to the small amount of matrix exposed at the fracture face.

Although the fatigue properties of the composite were very good, reflecting the high fatigue resistance of the fibres themselves, fatigue testing was unique in introducing new characteristics to the composite fractures. A noticeable increase was found in the proportion of fibre failures initiated at the fibre surface, suggesting that the presence of matrix fatigue cracks weakened the fibres, possibly by a stress-concentration effect. In addition, interfacial weaknesses were exposed by fatigue testing, both at the fibre/matrix interface and at interfaces between foils in the matrix.

Acknowledgements

Thanks are due to the following colleagues; A. Maybury (sonic modulus testing), G. Booty (impact testing), B. A. Proctor, F. P. Mallinder, J. W. Johnson and K. T. Kedward (useful discussions).

The permission of Rolls-Royce Limited to publish the paper is gratefully acknowledged.

References

1. A. KELLY, and G. J. DAVIES, *Met. Rev.* **10** (37), (1965) 1.
2. D. CRATCHLEY, *ibid* p. 79.
3. D. CRATCHLEY, A. A. BAKER, and P. W. JACKSON, *Mat. in. Des. Eng.* **64** (1966) 83.
4. R. V. SARA, 14th *SAMPE Symposium*, Nov. 1968.
5. M. J. NOONE, R. L. MEHAN, and W. H. SUTTON, Final Report: Contract N00019-68-C-0304 (Jan. 1969).
6. K. KREIDER and M. MARCIANO, *Trans. Met. Soc. AIME* **245** (1969) 1279.
7. J. F. DOLOWY, JR. and R. J. TAYLOR, 16th *SAMPE Symposium*, Sept. 1969.
8. H. SHIMIZU and J. F. DOLOWY, JR., *ASTM-STP*-460 (1969) 192.
9. L. W. DAVIS, P-159 835 (1969).
10. K. KREIDER and G. R. LEVERANT, 10th *SAMPE Symposium*, Nov. 1966.
11. E. M. BREINAN and K. G. KREIDER, *Met. Trans.* **1** (1970) 93.
12. K. C. ANTONY and W. H. CHANG, *Trans. ASM* **61** (1968) 550.
13. D. M. SCHUSTER, and R. P. REED, *J. Composite Materials* **3** (1969) 562.
14. R. C. JONES, *ASTM-STP*-460 (1969) 512.
15. R. P. I. ADLER and M. L. HAMMOND, *Appl. Phys. Letters* **14**, 11 (1969) 354.
16. P. E. CHEN and J. M. LIN, *Mat. Res. Standards* **9** (1969) (8), 29.
17. A. A. BAKER and D. CRATCHLEY, *Appl. Mat. Res.* **3** (1964) 215.
18. A. A. BAKER, *J. Mater. Sci.* **3** (1968) 412.
19. A. A. BAKER and D. CRATCHLEY, *Appl. Mat. Res.* **5** (1966) 92.
20. M. SALKIND and V. PATARINI, *Trans. Met. Soc. AIME* **239** (1967) 1268.
21. P. C. PARIS, in "Fatigue: an Interdisciplinary Approach" (eds. J. J. Burke, N. L. Reed and V. Weiss (Syracuse University Press, 1964). (from Proc. 10th Sagamore Army Materials Research Conf.).

Received 10 March and accepted 20 March 1971.